Journal of Crohn's and Colitis, 2020, 1473–1487
doi:10.1093/ecco-jcc/jjaa085
Advance Access publication April 28, 2020
Original Article

Original Article

Enteroids Generated from Patients with Severe Inflammation in Crohn's Disease Maintain Alterations of Junctional Proteins

Michael Meir,[a] Jonas Salm,[a] Christina Fey,[b] Matthias Schweinlin,[b] Catherine Kollmann,[a] Felix Kannapin,[a] Christoph-Thomas Germer,[a] Jens Waschke,[c] Christopher Beck,[d] Natalie Burkard,[a] Marco Metzger,[b,e] Nicolas Schlegel[a]

[a]Department of General, Visceral, Transplant, Vascular and Pediatric Surgery, University Hospital Wuerzburg, Oberduerrbacherstrasse 6, 97080 Wuerzburg, Germany [b]Chair for Tissue Engineering and Regenerative Medicine, Roentgenring 11, 97070 Wuerzburg, Germany [c]Institute of Anatomy and Cell Biology, Ludwig-Maximilians-University, Pettenkoferstraße 11, 80336 Munich, Germany [d]Institute of Pathology, Josef-Schneider-Straße 2, 97080 Wuerzburg, Germany [e]Fraunhofer Institute for Silicate Research ISC, Translational Centre for Regenerative Therapies TLC-RT, Roentgenring 11, 97070 Wuerzburg, Germany

Corresponding author: Univ. - Prof. Nicolas Schlegel, MD, Department of General, Visceral, Transplant, Vascular and Pediatric Surgery, University Hospital Wuerzburg, Oberduerrbacherstrasse 6, 97080 Wuerzburg, Germany. Tel: +49 931 201 38217; Email: Schlegel_N@ukw.de

Abstract

Background: The mechanisms underlying loss of intestinal epithelial barrier [IEB] function in Crohn's disease [CD] are poorly understood. We tested whether human enteroids generated from isolated intestinal crypts of CD patients serve as an appropriate *in vitro* model to analyse changes of IEB proteins observed in patients' specimens.

Methods: Gut samples from CD patients and healthy individuals who underwent surgery were collected. Enteroids were generated from intestinal crypts and analyses of junctional proteins in comparison to full wall samples were performed.

Results: Histopathology confirmed the presence of CD and the extent of inflammation in intestinal full wall sections. As revealed by immunostaining and Western blot analysis, profound changes in expression patterns of tight junction, adherens junction and desmosomal proteins were observed in full wall specimens when CD was present. Unexpectedly, when enteroids were generated from specimens of CD patients with severe inflammation, alterations of most tight junction proteins and the majority of changes in desmosomal proteins but not E-cadherin were maintained under culture conditions. Importantly, these changes were maintained without any additional stimulation of cytokines. Interestingly, qRT-PCR demonstrated that mRNA levels of junctional proteins were not different when enteroids from CD patients were compared to enteroids from healthy controls.

Conclusions: These data indicate that enteroids generated from patients with severe inflammation in CD maintain some characteristics of intestinal barrier protein changes on a post-transcriptional level. The enteroid *in vitro* model represents an appropriate tool to gain further cellular and molecular insights into the pathogenesis of barrier dysfunction in CD.

Key Words: Inflammatory bowel disease, enteroid, intestinal epithelial barrier, inflammation, junctional complex, junctional proteins

1. Introduction

Mucosal healing and restoration of intestinal epithelial barrier [IEB] function in patients with inflammatory bowel diseases [IBD] critically contribute to improved outcomes of patients.[1,2] Therefore, it is widely accepted that IEB dysregulation plays a major role in the development and perpetuation of IBD.[3] While therapeutic options in IBD are confined to modulating the aberrant pathological immune response of patients, direct targeting of the dysfunctional IEB would be a promising approach to induce clinical remission. One of the main reasons for the lack of specific barrier-stabilizing therapies is the limited understanding of the mechanisms underlying loss of the IEB in IBD.

Maintenance of the IEB is primarily dependent on the integrity of the terminal bar, also known as apical junctional complex between enterocytes.[4,5] Sealing of the intercellular cleft is provided by tight junctions consisting of claudins and occludin, whereas intercellular adhesion is maintained by adherens junctions and desmosomes. Previously, it was reported that patients with Crohn's disease [CD] show altered tight junction integrity and loss of desmosomal adhesion while adherens junctions appear largely unaffected.[6–8] However, it is not clear whether these distributional changes of junctional proteins in CD are a consequence of or the cause for the inflammation seen in this disease.

Suitable models are needed to provide further insights into the mechanisms of IEB dysregulation in IBD. On the one hand, current murine *in vivo* models have the problem that they mimic the inflammatory phenotype but not the pathogenesis of IBD.[9–12] In addition, while the advantage of these *in vivo* models is to study the inflammatory reaction in the context of a living organism, the transfer from mouse to human remains problematic. On the other hand, there has been a lack of sufficient human *in vitro* models, as stable primary enterocyte cell cultures were not possible until recently.[13]

A novel option to overcome this problem arose with the possibility of growing intestinal epithelial cells from leucine-rich repeat-containing G-protein coupled receptor5-positive [Lgr5$^+$] stem cells to generate enteroids or colonoids in a three-dimensional structure.[14–17] With this technique, enterocytes can be cultured both from healthy donors and from patients with IBD. Previous studies have shown permanent changes in mRNA expression in enteroids that derived from areas of active inflammation of IBD patients, and these were consistent over multiple passages.[18,19] Notably, it was reported that enteroids from patients with IBD required additional stimulation with cytokines to maintain typical features of the disease.[20]

We hypothesized that enteroids from CD patients might be the ideal model to further determine the mechanisms underlying IEB dysregulation. However, because it is not known whether these enteroids serve as a suitable model in the context of epithelial barrier homeostasis, we performed a detailed analysis of the changes of junctional proteins in human enteroids. To determine between inherent changes and alterations due to culture conditions, we systematically compared enteroids from patients with CD to original tissue specimens from the same cohort of patients. Additionally, similar analyses were carried out with enteroids from donors who did not have IBD.

2. Materials and Methods

2.1. Human tissue samples

Human tissue samples were collected from patients with CD who had an indication for surgery [Table 1]. All tissue samples derived from the terminal ileum. They were obtained from the inflamed centre of the resection specimens as well as the resection margins, where no inflammation was seen. Control tissue samples derived from patients without IBD who required right hemicolectomy due to colon carcinoma, in which surgical resection routinely involves a part of the healthy terminal ileum distant to the carcinoma [Table 1]. All patients gave their informed consent prior to surgery and ethical approval was given by the Ethical Board of the University of Wuerzburg [proposal numbers 113/13, 46/11, 42/16].

2.2. Tissue processing

As outlined in Figure 1 the specimens from healthy donors were processed for enteroid generation. Enteroids from CD patients were generated from the resection margins [terminal ileum], where no inflammation was macroscopically seen, as well as from the centre of the resected specimens where inflammation was most pronounced. From each site, i.e. resection margin and centre of the specimens, corresponding full wall tissues were fixed in 4% paraformaldehyde [PFA] and snap frozen in liquid nitrogen.

2.3. Generation of enteroids

Intestinal epithelial cells were isolated from resected human full wall intestine, 1 cm^2 in size as described previously.[8,17] Importantly, all enteroids were generated and cultured in exactly the same way regardless of whether they originated from healthy donors or from CD patients. Briefly, villi were scraped off the muscle-free mucosa using a sterile glass slide. The remaining tissue was transferred into a 50-mL falcon tube with 20 mL of 4°C cold hanks balanced salt solution [HBSS] [Sigma-Aldrich], vortexed for 5 s and the supernatant discarded. This washing step was repeated until the supernatant was entirely cleared of cell debris. Afterwards, the tissue was incubated in 4°C cold 2 mM ethylenediaminetetraacetic acid [EDTA]/HBSS solution [Sigma-Aldrich] for 30 min at 4°C under gentle rotation on a shaker. Subsequently, the tissue was washed once in 20 mL HBSS by manually inverting the tube five times. The mucosa was then transferred into a new tube with 10 mL HBSS and shaken five times manually. This shaking procedure was repeated four times always using a new tube. Each solution was checked for the amount and size of crypts within drops under the microscope. The supernatants containing the most vital appearing crypts were pooled and centrifuged at 350 *g* for 3 min at room temperature [RT]. The pellet was resuspended in 10 mL basal medium, Dulbecco's modified Eagle's medium [DMEM]-F12 Advanced [Invitrogen] supplemented with 1× N2, 2× B27, 1× Anti-Anti, 10 mM 4-[2-hydroxyethyl]-1-piperazineethanesulfonic acid [HEPES], 2 mM GlutaMAX-I [all from Invitrogen], 1 mM *N*-acetylcysteine [Sigma-Aldrich], and the crypt number was estimated in a 10-µL drop by microscopic observation. Crypts were centrifuged in a non-stick 1.5-mL tube at 350 *g* for 3 min at RT and the supernatant was removed. The tube with the cell pellet was placed on ice until further use. The pellet was resuspended in an appropriate amount of cold Matrigel [Corning], i.e. 5000 crypts/mL. Drops of 50 µL per well were seeded in a 24-well plate and incubated for 10–20 min until the Matrigel was solidified. The culture medium contained a mixture of 50% fresh basal medium and 50% Wnt3A-conditioned medium.

Furthermore, the following growth factors were added: 500 ng/mL hR-Spondin 1, 50 ng/mL human epidermal growth factor [hEGF] [both PeproTech], 100 ng/mL rec Noggin [PeproTech], 10 mM nicotinamid, 10 µM SB202190, 10 nM [Leu15]-Gastrin I [all three Sigma-Aldrich], 500 nM A83-01 [Tocris Bioscience] and 500 nM LY2157299 [Axon MedChem]. Additionally, 10 µM Rho-kinase inhibitor Y-27632 [Tocris Bioscience] was added after seeding as well as each splitting. The cells were expanded as organoid/enteroid

Table 1. Patient characteristics [CD = Crohn's disease, Pat = patient, Cont = control, F = female, M = male]

	Sex	Age [years]	CD-related medication	Indication for surgery	Surgery
Pat01	F	51	6-Mercaptopurine	Small bowel obstruction	Laparoscopic ileocaecal resection
Pat02	M	57	Glucocorticoids	Interenteric fistula	Laparoscopic ileocaecal resection
Pat03	F	59	Methotrexate, sulfasalazine	Interenteric fistula	Open ileocaecal resection, strictureplasty
Pat04	F	30	6-Mercaptopurine, glucocorticoids	Refractory ileitis	Laparoscopic ileocaecal resection
Pat05	M	33	Glucocorticoids	Subtotal stenosis terminal ileum	Laparoscopic ileocaecal resection
Pat06	M	26	Adalimumab	Interenteric fistula	Open ileocecal and sigmoid resection
Pat07	F	53	Azathioprine, glucocorticoids	Chronic stenosis with interenteric fistula	Laparoscopic ileocaecal resection
Pat08	F	29	Glucocorticoids	Interenteric fistula	Laparoscopic ileocaecal resection
Pat09	F	28	6-Mercaptopurine, glucocorticoids	Refractory ileitis	Laparoscopic ileocaecal resection
Pat10	M	22	Vedolizumab, glucocorticoids	Severe colitis and fistulating proctitis	Right hemicolectomy, proctectomy
Pat11	M	27	Azathioprine	Interenteric fistula	Laparoscopic ileocaecal resection
Pat12	M	44	Glucocorticoids	Entero-sigmoid fistula	Open ileocaecal resection
Pat13	F	63	Mesalazine	Anastomotic stenosis post-ileocaecal resection	Ileoascendostomy resection
Pat14	M	46	Mesalazine	Anastomotic stenosis post-ileocaecal resection	Ileoascendostomy resection
Pat15	M	44	Glucocorticoids	Retroperitoneal and interenteric fistula	Right hemicolectomy
Pat16	F	23	Infliximab, glucocorticoids	Anastomotic stenosis post-ileocecal resection	Ileoascendostomy resection
Cont01	F	74	—	Caecal carcinoma	Hemicolectomy
Cont02	F	79	—	Caecal carcinoma	Hemicolectomy
Cont03	M	47	—	Descending colon perforation	Segmental ileum resection, left hemicolectomy
Cont04	F	92	—	Caecal carcinoma	Hemicolectomy
Cont05	M	74	—	Ascending colon polyps	Hemicolectomy
Cont06	M	86	—	Ascending colon carcinoma	Hemicolectomy
Cont07	M	62	—	Caecal polyps	Hemicolectomy
Cont08	M	72	—	Ascending colon polyps	Hemicolectomy
Cont09	F	78	—	Caecal carcinoma	Hemicolectomy
Cont10	M	68	—	Neuroendocrine tumour	Hemicolectomy
Cont11	M	84	-	Ascending colon carcinoma	Hemicolectomy
Cont12	M	76	-	Neuroendocrine tumour	Hemicolectomy
Cont13	F	68	-	Ascending colon carcinoma	Hemicolectomy
Cont14	F	61	-	Neuroendocrine tumour	Hemicolectomy

culture for 8–10 weeks. Enteroids for this study were used up to passage 25.

2.4. Immunocytochemistry/immunohistochemistry

The human specimens were embedded in paraffin and sectioned as 1-µm slices. The enteroids were digested from Matrigel with Cell Recovery Solution [Thermo Fisher] for 1 h on ice, washed with phosphate-buffered saline [PBS]$^-$ [Sigma Aldrich] and fixed with 4% PFA. After embedding in histogel [Thermo Fisher] the enteroids were also embedded in paraffin. Immunostaining was performed after removal of paraffin as described for epithelial monolayers and human specimens.[8,21] Then monolayers and tissue slides were incubated at 4°C overnight using the following primary antibodies at 1:100 in PBS [Sigma-Aldrich]: rabbit anti-Desmoglein2 [Merck Milipore], rabbit anti-Desmocollin2 [Invitrogen], mouse anti-E-Cadherin [BD Biosience] and mouse anti-Claudin1, 2, 4, 5 [Invitrogen]. As secondary antibodies, we used Cy3- or 488-labelled goat anti-mouse, goat anti-rabbit, or mouse anti-goat [all diluted 1:600, Dianova]. Controls were only incubated with secondary antibodies to exclude unspecific staining patterns [Supplementary Figure 4]. Coverslips and filters were mounted on glass slides with Vector Shield Mounting Medium as anti-fading compound, which included 4′,6-diamidin-2-phenylindol [DAPI] to stain cell nuclei additionally [Vector Laboratories]. Representative experiments were imaged with a fluorescence microscope [BZ-9000; BIOREVO] and a confocal microscope [Leica TCS SP2]. To provide an objective evaluation of the changes of junctional proteins at the cell borders, pictures from immunostaining were quantified using ImageJ [National Institutes of Health] by a blinded investigator as described previously[22]: a 10-µm line was placed perpendicular to the cell border with the cell border representing the middle of this line. Thereafter the relative distribution of fluorescence pixel intensity was measured, which resulted in a curve with a maximum peak in the middle of the graph if the cell junction was intact. Accordingly, loss of staining intensity at the cell borders resulted in a flattening of the curve [Supplementary Figures 2 and 3]. For each sample at least four randomly chosen junctions were measured, followed by statistical analysis.

2.5. Western blotting

For Western blot analysis of enteroids, the Matrigel was digested with Cell Recovery Solution [Thermo Fisher] for 1 h on ice before being centrifugated for 3 min at 300 *g*, washed with PBS$^-$ [Sigma Aldrich] and homogenized in sodium dodecyl sulfate [SDS] lysis buffer containing 25 mM HEPES, 2 mM EDTA, 25 mM NaF and 1% SDS. To analyse human enterocytes from full wall lysates, the mucosa was mechanically dissected from the underlying tissue immediately after the resection.

The specimens were then lysed in SDS lysis buffer using TissueLyser [Qiagen]. SDS gel electrophoresis and blotting were carried out after normalization of the protein amount using a bicinchoninic acid assay [BCA] [Thermo Fisher] as described previously.[21] The primary antibodies rabbit anti-Desmoglein2 [Life Technologies], rabbit anti-Desmocollin2 [Invitrogen], mouse anti-E-Cadherin [BD Bioscience] and mouse anti-Claudin1, 2, 4, 5 [all

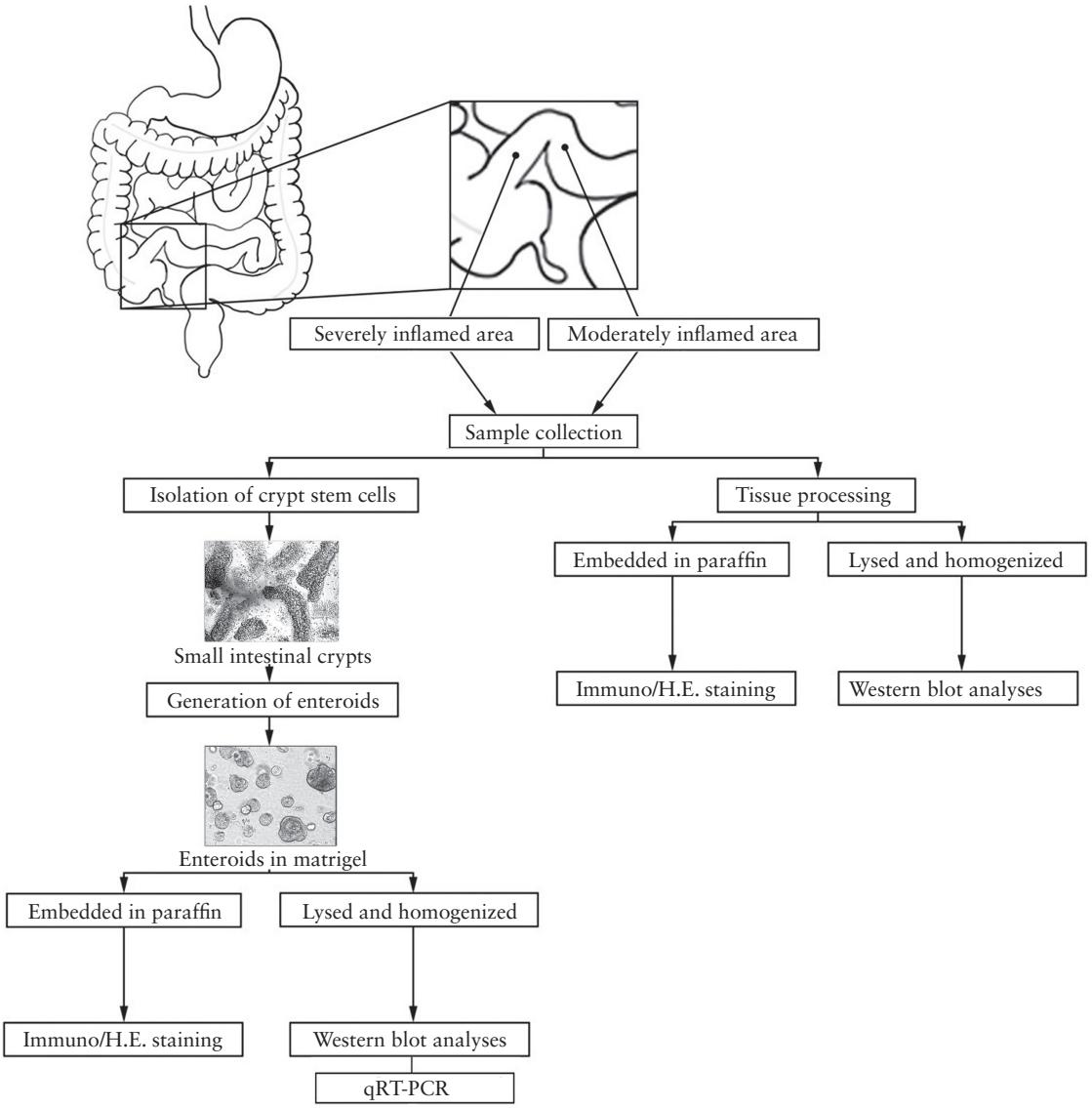

Figure 1. Schematic overview to demonstrate tissue processing after resection of CD samples: tissue samples from patients with CD were taken from the centre of the specimen that appeared macroscopically inflamed, or from the resection margins that appeared to be macroscopically non-inflamed. One part of the tissue was then used for the generation of enteroids, while the other was used to investigate the tissue as full wall sample.

Invitrogen] were used at a dilution of 1:1000 in 5% bovine serum albumin [BSA] and 0.1% Tween. As secondary antibodies, horseradish peroxidase-labelled goat anti-rabbit IgG and goat anti-mouse IgG [both Santa Cruz Biotechnology] were used [1:3000 in 5% BSA, 0.1% Tween]. To validate normalization, peroxidase-labelled β-Actin [Sigma-Aldrich] antibodies were applied. Chemiluminescence signal detection and quantification were performed by densitometry [ChemicDoc Touch Bio-Rad Laboratories]. Optical densities [OD] were quantified in each Western blot using Image Lab [ChemicDoc Touch Bio-Rad Laboratories] for statistical evaluation.

2.6. Quantitative real-time PCR

For RNA isolation from enteroids, nine wells of a 24-well plate were resuspended in 500 µL Cell Recovery Solution [Corning] per well and placed on ice for 1 h. Before the enteroids were lysed in RLT buffer [Invitrogen Life Technologies], they were centrifuged at 300 *g* for 3 min and washed with PBS [Sigma-Aldrich]. Total RNA was extracted using the RNeasy Mini Kit [Qiagen] according to the manufacturer's instructions. RNA integrity was verified using the Experion automated electrophoresis station from Bio-Rad Laboratories before measuring RNA concentration at 260 nm [Nano Drop 2000c, Thermo Fisher Scientific]. For first-strand cDNA synthesis, 1 µg total RNA was employed using the iScript cDNA synthesis kit from Bio-Rad Laboratories. The cDNA synthesis of 1:5 diluted cDNA was performed by heating the probes at 25°C for 5 min, at 42°C for 30 min and at 85°C for 5 min. Quantitative PCR [qPCR] was performed with MESA Green qPCR MasterMix Kit for SYBR Green containing MeteorTaq hotstart DNA polymerase [Eurogentic GmbH]. The following primer pairs were used:

Claudin1: forward 5′-GCGCGATATTTCTTCTTGCAGG-′3, reverse 5′-TTCGTACCTGGCATTGACTGG-′3
Claudin4: forward 5′-CCCCGAGAGAGAGTGCCCTG-′3, reverse 5′- AGCGTCCACGGGAGTTGAGGA-′3

Claudin5: forward 5′-CCATGGGATGAGAGAGACAG-′3, reverse 5′-CTGACCAAGGTTTGCAGAAG-′3
Claudin2: forward 5-′CTCCCTGGCCTGCATTATCTC-′3, reverse 5′- ACCTGCTACCGCCACTCTGT-′3
Dsg2: forward 5′-AACGACAACTGTCCCACACT-′3, reverse 5′-TTTCTTGGCGTGCTATTTTC-′3
Dsc2: forward 5′-ATACAGCAGCACGTCTTTCC-′3, reverse 5′-CCAATCCTTGGATCTACACG-′3

The qPCRs were performed on a CFX96 real-time PCR system [Bio-Rad Laboratories] operated by CFX Manager Software [version 3.0, Bio Rad Labaratories]. The cycler protocol was 5 min at 95°C, 40 cycles with 15 s at 95°C, 60 s at 60°C and 5 min at 72°C. Expression was normalized to the reference gene β-actin and -fold expression was calculated with the ΔΔCq method.

2.7. Histopathological grading of the full wall tissue samples

Enteroids and full wall tissue specimens embedded in paraffin were stained with haematoxylin and eosin [H&E] so that the presence of CD and the level of inflammation could be verified by a blinded pathologist using a modified score[23]: 1 = no inflammation [mucosa was free of inflammation, there was no sign of erosion or lymphocyte infiltration]; 2 = moderate inflammation [epithelium was intact but showed signs of oedema, interstitial haemorrhage or significant lymphocyte infiltration]; 3 = severe inflammation [surface of the mucosa was often irregular, breaches in the epithelium were seen, severe lymphocyte infiltration, formation of granulomata]. A representative image for each score is shown in Figure 2.

2.8. Statistics

Statistical analysis was performed using Prism [GraphPad Software]. Data are presented as means ± SE. Statistical significance was assumed at $p < 0.05$. A paired Student's t-test was performed for two-sample group analysis after checking for a Gaussian distribution [as validated by D'Agostino-Pearson's normality test]. Analysis of variance [ANOVA] followed by Tukey's multiple comparisons test and Bonferroni correction was used for multiple sample groups.

3. Results

3.1. Patient characteristics and histopathological grading of full wall specimens

Human tissue samples were collected during surgery from patients with ileitis terminalis in CD. Indication for surgery was conservative refractory CD or complications of CD as listed in Table 1. Terminal ileum samples of controls were obtained from patients who required right hemicolectomy but did who did not have IBD.

Due to the different indications for surgery, the age of the patient cohorts differed significantly between controls and patients with CD, although younger adults as well as very old patients were excluded from the study to minimize any age-dependent bias. The mean age of controls was 71.6 ± 3.6 years compared to 39.8 ± 3.5 years in CD patients with a comparable sex distribution in both groups. As outlined above, tissue samples for enteroid generation and full wall tissues were collected from the resection margins [terminal ileum] as well as from the centre of the specimens [Figure 1].

In a first step, H&E stainings of full wall tissue samples from both areas were investigated morphologically and inflammation was assessed using a previously published scoring system for IBD.[23] This

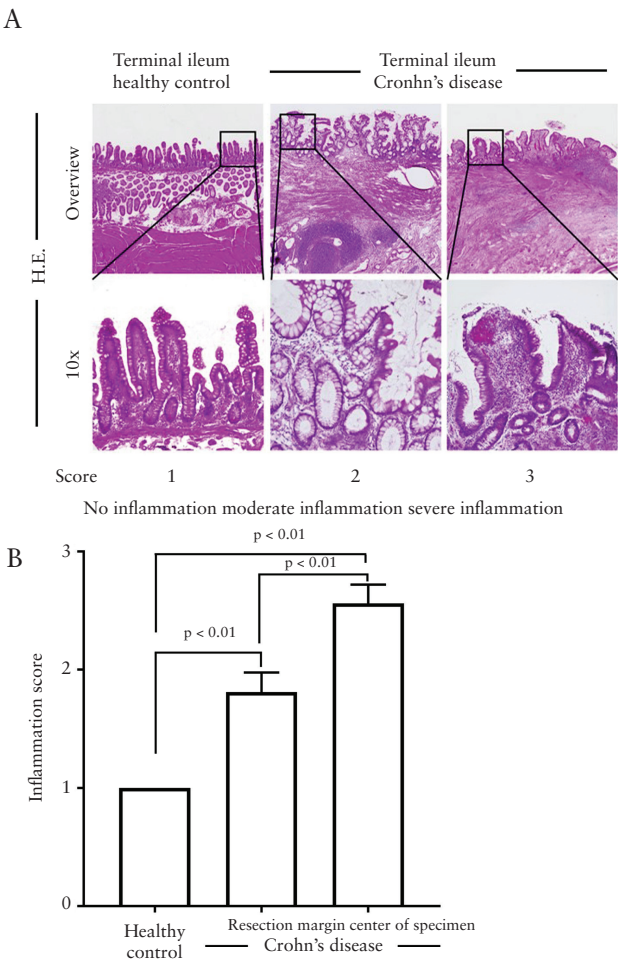

Figure 2. Histopathological evaluation of inflammation. [A] H&E-stained images exemplifying the scoring system on which histopathological analysis was carried out, from 1 [no inflammation] to 3 [severe inflammation]. [B] The results of histopathological scoring. This confirmed that patients without IBD showed no inflammation whereas samples from CD patients taken from the centre of the specimens mostly displayed severe inflammation of 2.6 ± 0.2 while in samples from the resection margins the inflammation score was signifcantly lower, 1.8 ± 0.2 [$n = 16$; $p < 0.01$].

aimed to verify the presence of CD and to grade the extent of inflammation in the different samples [Figure 2A]. Histopathological analysis from patients without IBD showed no signs of inflammation, whereas patients with CD who underwent surgery showed significantly increased inflammation scores. As demonstrated in Figure 2B inflammation was significantly more pronounced in the centre of the tissue specimens from CD patients [2.6 ± 0.2] than at the resection margins [1.8 ± 0.2; Figure 2].

3.2. Characterization of junctional changes in specimens from CD

Next, we analysed changes of the tight junction proteins Occludin, and Claudin1, 2, 4 and 5 using immunostaining and Western blot analyses. In immunostaining of full wall sections from patients without IBD, tight junction proteins Claudin1 [Figure 3A], Claudin4 [Figure 3B] and Claudin5 [Figure 3C] were regularly distributed at the cell borders in the epithelial layer. In specimens from patients with CD, an overall reduction of Claudin1 [Figure 3A], Claudin4 [Figure 3B] and Claudin5 [Figure 3C] at the cell borders was

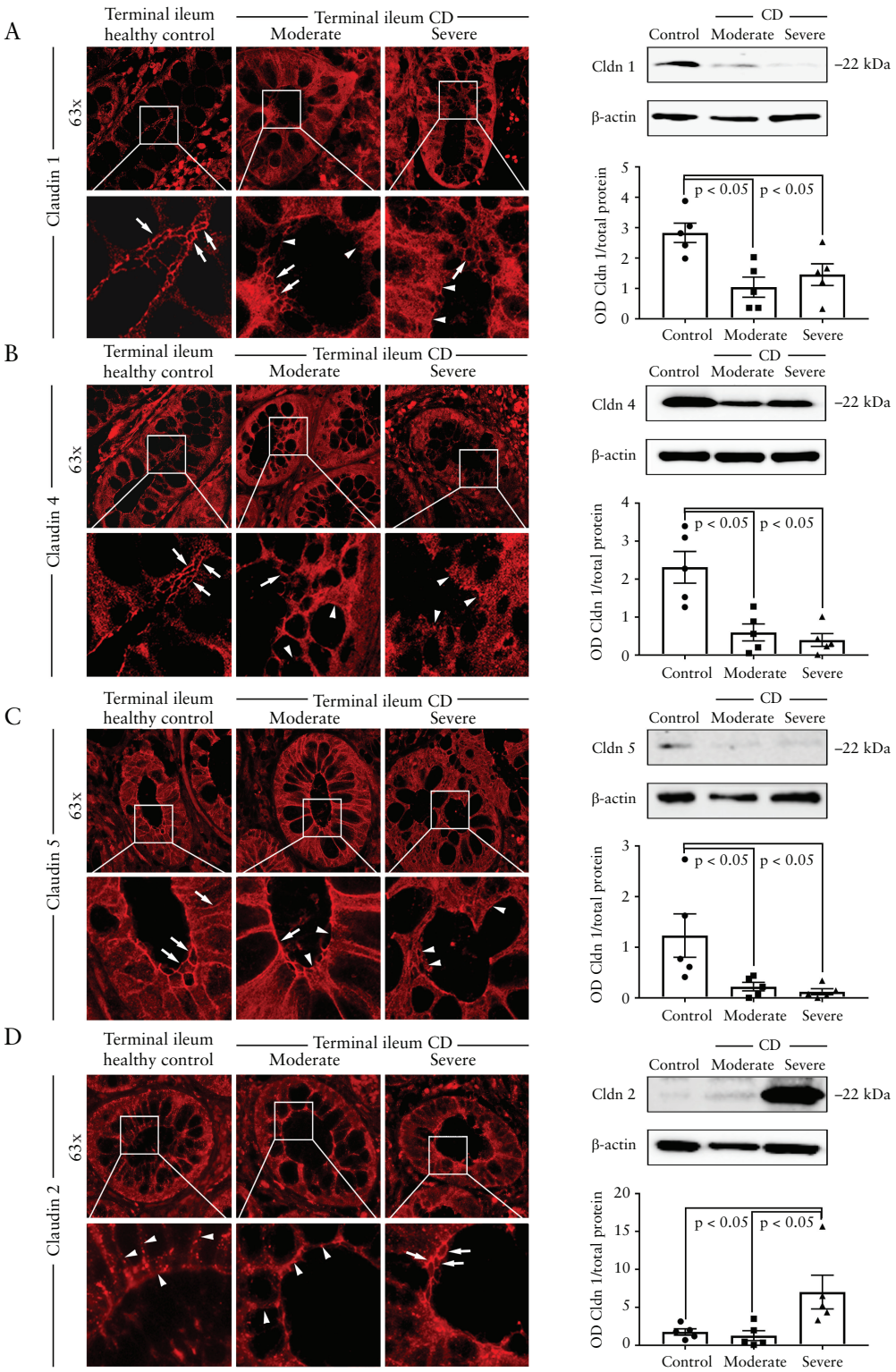

Figure 3. Distribution and amount of Claudins is altered in patients with CD. Immunostaining [left side] and Western blots [right side] for different Claudins were performed. Arrows indicate examples of intact staining patterns of the respective junctional protein in intestinal epithelial cells; arrowheads point to areas where the specific staining pattern is lost in epithelial cells. Data for Western blot quantifications are presented as raw values [protein of interest/total protein amount]. [A] Claudin1 was regularly distributed at the cell borders in healthy control specimens and was reduced in the moderately and severe inflamed mucosa of patients with CD. Western blots showed significantly reduced levels of Claudin1 [representative images are shown for $n = 16$ immunostaining and $n = 5$ Western blot analyses, $p < 0.05$]. [B] Barrier-stabilizing Claudin4 was reduced dependent on the extent of inflammation in immunostaining and signficantly reduced in Western blot analysis [representative images are shown for $n = 16$ immunostaining and $n = 6$ Western blot analyses, $p < 0.05$]. [C] Immunostaining showed reduced Claudin5 at the cell borders in CD patients. Western blots confirmed a significant reduction of Claudin5 in moderately and severely inflamed tissue [representative images are shown for $n = 16$ immunostaining and $n = 6$ Western blot analyses, $p < 0.05$]. [D] Pore-forming Claudin2 that was barely visible at the cell borders under control conditions was clearly present at the cell borders in severely inflamed tissue in CD patients. In Western blots, Claudin2 was significantly upregulated in the severely inflamed tissue specimens [representative images are shown for $n = 16$ immunostaining and $n = 5$ Western blot analyses, $p < 0.05$].

apparent. Accordingly, quantifications of the immunostaining showed a significant reduction of the immunostaining signal for Claudin1, 4 and 5 in the severe inflamed specimen compared to healthy controls [Supplementary Figure 2A, C, D]. For Claudin1 and 4, in particular, the extent of the loss at the cell borders correlated with the severity of inflammation [Supplementary Figure 2A, C]. Similarly, Western blot analyses of patients' tissue samples showed a reduction of the protein levels of Claudin1, 4 and 5 in the moderately and severely inflamed mucosa compared to healthy controls. In the severely inflamed tissue, Claudin1 was significantly reduced to 51.4 ± 12.5% of protein levels in control samples [Figure 3A]. In severely inflamed tissue, Claudin4 was decreased to 17.3 ± 7.2% [Figure 3B] and Claudin5 was reduced to 9.8 ± 4.8% of controls [Figure 3C]. Pore-forming tight junction protein Claudin2, which is usually upregulated in inflammation, was hardly visible in the enterocyte layer in control samples [Figure 3D] as well as in patients' samples with moderate inflammation. However, in severe inflammation Claudin2 was significantly upregulated to 310 ± 14% as seen at the cell borders [Figure 3D; Supplementary Figure 2B]. Similar results were obtained in Western blot analyses, where in the severely inflamed tissue Claudin2 was elevated to 398.5 ± 126.4% of controls.

For the tight junction protein Occludin comparable staining patterns were found in healthy control samples and in samples from patients with CD, both with moderate and with severe inflammation [Figure 4A; Supplementary Figure 2H]. Accordingly, Western blotting showed no significant differences when comparing samples from healthy patients to samples from CD patients [Figure 4A].

We additionally analysed the expression of adherens junction protein E-Cadherin [E-Cad] as well as desmosomal proteins Desmoglein2 [Dsg2] and Desmocollin2 [Dsc2] by immunostaining and Western blotting [Figure 4B–D]. E-Cad was found to be regularly distributed along the cell borders in healthy tissue sections and in CD patients with moderate inflammation [Figure 4B]. In patients' samples showing inflammation, loss of E-Cad was evident in most parts of the mucosa dependent on the extent of inflammation, and quantification of immunostaining revealed a significant reduction of the intensity of the fluorescence signal [Supplementary Figure 2G]. Western blot analysis demonstrated significant reduction of total protein levels of E-Cad in patients with CD [Figure 4B]. In immunostaining for Dsg2 [Figure 4C] and Dsc2 [Figure 4D], both desmosomal proteins were found to be regularly distributed along the cell borders of enterocytes in patients without IBD, whereas a significant loss of both Dsg2 and Dsc2 was observed in moderately and severely inflamed sections [Supplementary Figure 2E, F]. Accordingly, Western blot analyses of severely inflamed tissue showed a decrease of Dsg2 and Dsc2 to 29.0 ± 14.5 and 28.5 ± 15.5% when compared to controls.

3.3. Enteroids from patients with CD maintain changes of junctional proteins observed in patients' full wall tissue samples

Enteroids from five severely inflamed specimens, five moderately inflamed areas of the patients analysed previously and five control patients were generated. The *in vitro* culture of enteroids was feasible in all groups. After isolation of crypt units from the terminal ileum, all enteroids showed similar morphology in the H&E staining [Figure 5], although they grew much slower in the first passages when compared to enteroids from healthy patients. This was no longer evident after passage 9. Of note, we lost a number of samples of IBD patients due to a higher number of microbial contaminations in the culture. As outlined in the Material and Methods, all enteroids from CD patients were generated under the same conditions as enteroids from healthy donors (i.e. without additional cytokine stimulation).

We characterized potential changes of junctional proteins in enteroids from healthy donors and in enteroids from patients with CD. The enteroids from healthy donors showed regular staining patterns for Claudin1 [Figure 6A], Claudin4 [Figure 6B], Claudin5 [Figure 6C] and Occludin [Figure 7A], whereas Claudin2 was only sparsely found [Figure 6D] at the cell borders of enterocytes [Supplementary Figure 3]. These observations matched the findings in full wall tissue. In contrast to the evaluation of full wall samples, Claudin1 was not changed in enteroids from moderately or severely inflamed tissue specimens of CD patients by immunostaining or Western blotting [Figure 6A; Supplementary Figure 3A]. However, Claudin2, 4 and 5 showed concordant significant down- and upregulation in enteroids when compared to overall changes of patients' full wall samples [Figure 6B, C; Supplementary Figures 3A, C]. The loss of Claudin5 in Western blots paralleled the results in human specimens where the concentration of Claudin5 was reduced to 32.2 ± 10.2% of controls while quantification of immunostaining only showed a trend towards reduced Claudin5 in the enteroids derived from severely inflamed specimen [Figure 6D; Supplementary Figure 3D]. This congruence was also observed for Occludin, where no changes were detected in enteroids from CD patients [Figure 6A; Supplementary Figure 3H]. For desmosomal cadherins Dsg2 and Dsc2 [Figure 7C, D], which were regularly distributed along the cell borders in control enteroids, a decrease was found in immunostaining of enteroids from tissue samples with moderate and severe inflammation. Quantification of the immunostaining showed that this was significant for Dsg2 but not for Dsc2 [Supplementary Figure 3E, F]. Similarly, Western blot analyses of the enteroids showed a significant reduction of protein levels of Dsg2 to 54 ± 10% of controls. The protein levels of Dsc2 showed a reduction to 58.4 ± 27.3% of controls, which was not significant due to heterogeneity of the Western blots. Nonetheless, these observations were comparable to the decrease of Dsg2 and Dsc2 observed in full wall tissue of CD patients. In contrast, E-Cad distribution at the cell borders was similar when comparing enteroids from healthy donors to enteroids from CD patients with moderate and severe inflammation [Figure 7B; Supplementary Figure 3G]. This was confirmed by Western blot analysis, where E-Cad levels were comparable in enteroids from healthy donors and CD patients. An overview comparing the overall changes observed in full wall tissues and in enteroids is provided in Table 2. In summary, these data demonstrated that enteroids generated from inflamed tissue of CD patients on average show alterations of junctional proteins without stimulation with cytokines.

Additionally, directly compared the enteroids to their corresponding full wall samples to detect whether each enteroid exactly reflects the same phenotype compared to its origin [Supplementary Figure 1]. Comparable to the observation made in the overall analysis, changes of E-Cad and for Claudin1 did not match in any case. For the other proteins analysed the enteroids largely reflected the situation in the full wall samples. In particular, for tight junction proteins Claudin4 [4/5 congruent in moderate inflammation, 5/5 in severe inflammation], Claudin5 [4/5 congruent in moderate inflammation, 4/5 in severe inflammation], Claudin2 [3/5 congruent in moderate inflammation, 5/5 in severe inflammation] and Occludin [5/5 in all cases] there was a high rate of matches. This was more heterogeneous for desmosomal proteins Dsg2 [1/5 congruent in moderate inflammation, 4/5 in severe inflammation] and especially for Dsc2 [2/5 congruent in moderate inflammation, 3/5 in severe inflammation]. This supported the impression that enteroids that were generated from sites of severe inflammation overall maintained their phenotype when compared to their original sample.

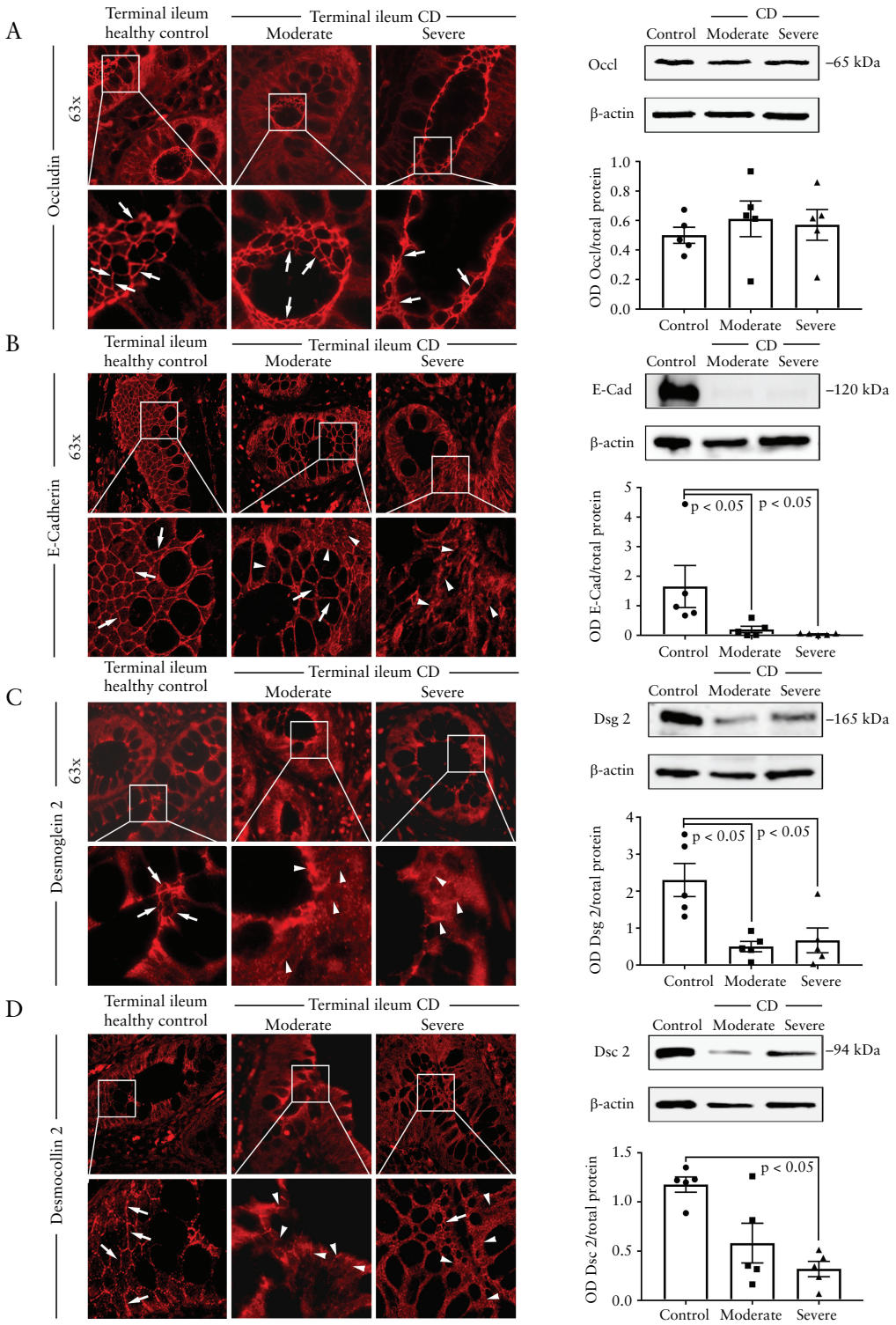

Figure 4. Changes of distribution and levels of Occludin, adherens junction and desmosomal proteins and Occludin in CD. Immunostaining [left side] and Western blots [right side] for Occludin, E-Cadherin and desmomal proteins Desmocolin2 and Desmoglein2 are shown. Arrows indicate intact examples for staining patterns of the respective junctional protein in intestinal epithelial cells, while arrowheads point to areas where the specific staining pattern is lost in epithelial cells. Data for Western blot quantifications are presented as raw values [protein of interest/total protein amount]. [A] The distribution and concentration of Occludin was not changed in the moderately or severely inflamed areas. No changes were observed in Western blot analyses in CD patients [representative images are shown for $n = 16$ immunostaining and $n = 6$ Western blot analyses, $p < 0.05$]. [B] E-cadherin was regularly distributed along the cell borders in healthy tissue in controls and was reduced when inflammation was more pronounced. In Western blot analysis E-cadherin was significantly reduced in CD patients with moderate and severe inflammation [representative images are shown for $n = 16$ immunostaining and $n = 5$ Western blot analyses, $p < 0.05$]. [C] Immunostaining of desmosomal protein Dsg2 demonstrated a reduction in moderately and severely inflamed sections from CD patients compared to controls. Accordingly, Western blot analyses showed a significant loss of Dsg2 compared to controls in moderate and severe inflammation [representative images are shown for $n = 16$ immunostaining and $n = 5$ Western blot analyses, $p < 0.05$]. [D] In immunostaining, Dsc2 was reduced in severely and moderately inflamed tissue compared to healthy terminal ileum. In Western blots the protein levels of Dsc2 were significantly reduced in CD samples from severely inflamed tissue [representative images are shown for $n = 16$ immunostaining and $n = 5$ Western blot analyses, $p < 0.05$].

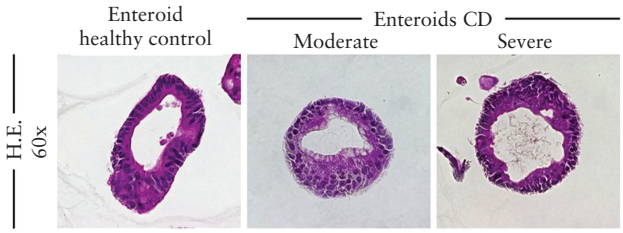

Figure 5. H&E staining from enteroids. Representative imagess H&E staining of enteroids generated from healthy donors and from patients with CD are shown. No obvious alterations were visible between the different donors and donor sites at this level.

3.4. qRT-PCR in enteroids showed unaltered expression patterns of Claudin2, Claudin 4, Dsg2 and Dsc2

To test whether the observed changes of junctional proteins in enteroids were evident on mRNA levels, we performed qRT-PCR for the junctional proteins, in which changes of the protein levels were most pronounced. However, we observed no difference in mRNA levels of Claudin2, Claudin4, Dsg2 and Dsc2 in enteroids from patients with CD when compared to enteroids from healthy patients [Figure 8]. This indicates a fixed manifestation of CD-dependent modifications on a post-transcriptional level.

4. Discussion

In the present study, a detailed characterization of IEB protein changes that are usually observed in patients with CD was carried out in surgical samples from patients with and without CD. The changes of junctional proteins were compared to the characteristics of enteroids generated from intestinal crypts of the same cohort of patients. As supported by previous studies, our data confirm that junctional proteins that are responsible for IEB function such as tight junctions, adherens junctions and desmosomes are significantly altered in full wall tissue specimens of CD patients. Interestingly, enteroids generated from patients with CD generally maintain a comparable distribution pattern of up- and down-regulation of junctional proteins when compared to full wall tissue samples. This was especially so when enteroids had been generated from sites of severe inflammation. It is important to emphasize that these changes were present without additional stimulation with proinflammatory cytokines or endotoxins. In summary, this confirms our primary hypothesis that enteroids from patients with CD represent a suitable *in vitro* model for further investigations on the pathogenesis of IEB alterations. Furthermore, because these enteroids were generated from crypts containing stem and progenitor cells of CD patients, these findings suggest a conserved pattern of changes of junctional proteins within the intestinal regeneration niche or on a stem level, respectively. This supports the view that inflammation-induced barrier defects in CD are not a secondary phenomenon due to an inappropriate immune response but play a primary role in the pathogenesis of CD,[24] which may be established on the level of intestinal stem cells.

4.1. Tight junctions, adherens junctions and desmosomes show a distinct pattern of changes in severe and in moderate inflammation in CD patients when compared to healthy individuals

In general, a distinct pattern of profound changes of junctional proteins has been amply described in previous studies in patients with IBD.[3] Most previous investigations on this topic focused on potential alterations of tight junction integrity. Accordingly, in the specimens of patients with CD we found a profound change in the expression and distribution of the barrier-sealing tight junction proteins. Claudin1, 4 and 5 were reduced while pore-forming Claudin2 was increased and Occludin was unchanged. This supports previous findings that reported profound changes in tight junction composition in patients with CD.[25] Nonetheless, similar to our previous reports in our patients we detected loss of Claudin1. This was not consistently reported in the literature, where increased Claudin1 expression and Occludin levels in CD patients have also been described.[26–28] It can be speculated that the specimens used in these earlier studies could have derived from patients with a longer duration of inflammation compared to our collective. In this context it has been observed that long-term inflammation leads to an overexpression of Claudin1 in colonic CD and is then associated with colorectal cancer.[26,29] However, it must be emphasized that CD-associated cancer is rarely found. Similarly, the fact that Occludin knock-out mice show no phenotype of barrier dysfunction of the intestinal epithelium, but an epithelial hyperplasia,[30] may point to a longer inflammation of the tissue used in the previous studies.

In our present data loss of adherens junction protein E-Cad in patients' samples with CD was especially found in severe inflammation, which is in line with previous observations,[6,31] while others reported that basal E-Cad polymorphisms in CD contribute to a mislocalisation of E-Cad.[32]

A relatively new observation is that desmosomal integrity is compromised in patients with CD.[6–8,33] This is supported by our data as all patients showed a profound loss of desmosomal proteins Dsg2 and Dsc2 in CD. In this context, it is interesting to note that changes of desmomosal integrity have attracted increasing attention because it has been recognized that especially Dsg2 in the intestine is involved in modulating signalling pathways regulating proliferation[34–36] and apoptosis.[37] Furthermore Dsg2 is a target for infective pathogens such as adenoviruses[38,39] or enteropathogenic *Escherichia coli*.[40]

A limitation of the comparison of patients with CD and healthy individuals in this study is the different age of the control specimens compared to the patients with CD due to the different indication for surgery. However, because barrier function is reduced in elderly patients, it can be assumed that the differences in junctional protein expression in healthy individuals compared to patients with CD would be even more pronounced when samples from patients of the same age were to be compared.[41] Nonetheless, the present data from patients' specimens provide further evidence for a distinct pattern of changes of different intestinal junctional proteins in CD.

4.2. Enteroids from patients with CD maintain characteristics of barrier alterations under culture conditions without additional stimulation with cytokines

The generation of enteroids or organoids from intestinal stem cells is increasingly recognized as a valuable model to investigate mechanisms of enterocyte function in health and disease.[14–17] However, it must be emphasized that the use of enteroids represents only one aspect contributing to the complex character of CD, and neglects the large contribution of an aberrant immune response as well as the potential influence on environmental factors and microbiota.[42]

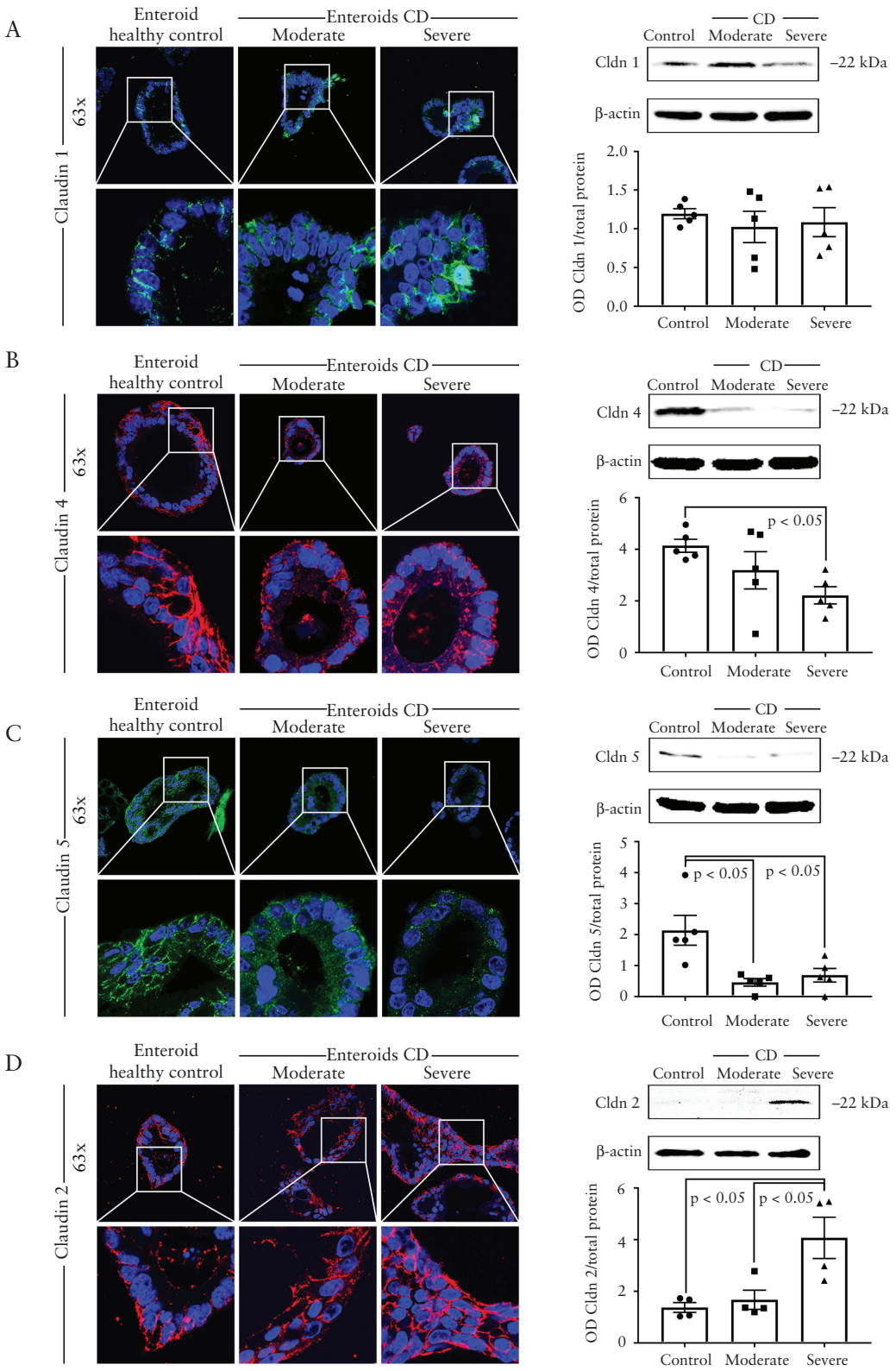

Figure 6. Distribution and levels of Claudins in enteroids are comparable to those seen in the orginal specimen. Immunostaining [left side] and Western blots [right side] are shown. Data for Western blot quantifications are presented as raw values [protein of interest/total protein amount]. [A] Immunostaining and Western blots showed no significant change in the distribution and levels of Claudin1 in inflamed specimens compared to healthy controls; [representatives are shown for $n = 5$, $p < 0.05$]. [B] In enteroids from CD patients from moderately and severely inflamed tissue, Claudin4 was reduced in immunostaining and Western blot analyses [[representatives are shown for $n = 5$, $p < 0.05$]. [C] Immunostaining and Western blots of Claudin5 showed a reduction in enteroids from moderately and severely inflamed CD patients [representatives are shown for $n = 5$, $p < 0.05$]. [D] Claudin2 was upregulated in enteroids from CD patients in immunostaining and in Western Blot analyses [representatives are shown for $n = 5$, $p < 0.05$].

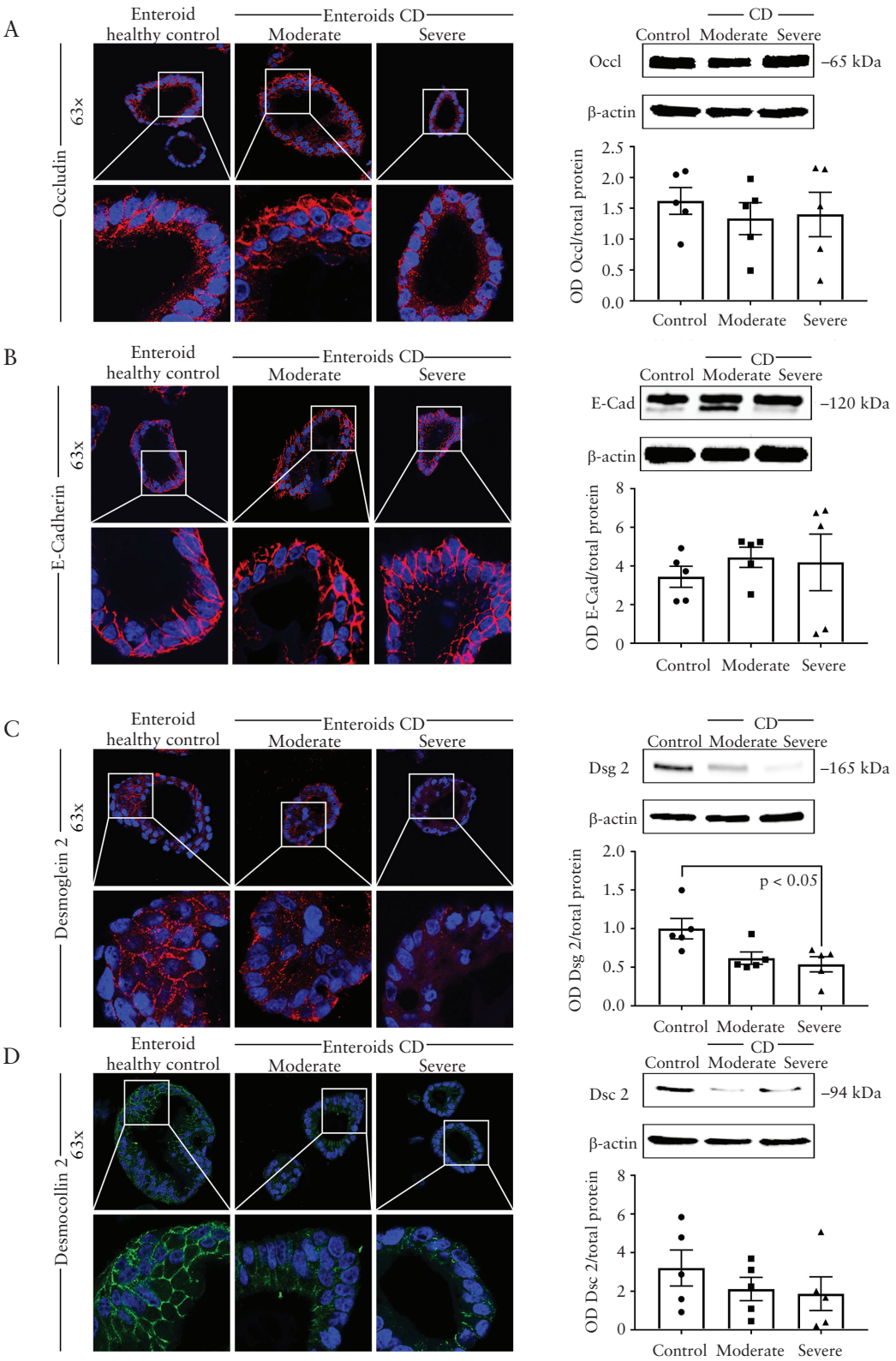

Figure 7. Changes of desmosomal proteins and E-cadherin in enteroids from patients with CD. Immunostaining [left side] and Western blots [right side] are shown. Data for Western blot quantifications are presented as raw values [protein of interest/total protein amount]. [A] Immunostaining and Western blots for Occludin were not altered in enteroids from moderately and severely inflamed areas of CD patients [representatives are shown for $n = 5$, $p < 0.05$]. [B] Protein levels of E-cadherin and immunostaining revealed no significant changes in the CD enteroids compared to enteroids from healthy controls [representatives are shown for $n = 5$, $p < 0.05$]. [C] Dsg2 was reduced in enteroids from moderately and severely inflamed specimens in immunostaining and Western blots [representatives are shown for $n = 5$, $p < 0.05$]. [D] Dsc2 was reduced in the enteroids from CD patients in immunostaining and in Western blots [representatives are shown for $n = 5$, $p < 0.05$].

Table 2. Overview to summarize the changes observed in full wall tissue [FWT] and enteroids [ENT] [• normal basal expression; ◦ no basal expression; ↓ reduced expression compared to controls; ↑ increased expression compared to controls].

Junctional proteins	Healthy control		Moderate inflammation		Severe inflammation	
	FWT	ENT	FWT	ENT	FWT	ENT
Claudin1	•	•	↓	•	↓	•
Claudin4	•	•	↓	•	↓	↓
Claudin5	•	•	↓	↓	↓	↓
Claudin2	◦	◦	◦	◦	↑	↑
Occludin	•	•	•	•	•	•
E-cadherin	•	•	↓	•	↓	•
Desmoglein2	•	•	↓	•	↓	↓
Desmocollin2	•	•	↓	•	↓	•

We decided to generate enteroids from resection specimens of patients with CD in comparison to enteroids from individuals not having IBD and to their respective full wall tissues to verify that this may be an appropriate model to further elucidate the mechanisms underlying loss of IEB function. Unexpectedly, we found in enteroids generated from CD patients that in an overall comparison the pattern of changes of junctional proteins was comparable to that found in full wall specimens. However, a more detailed comparison revealed that not each enteroid completely reflected the changes observed in its corresponding full wall sample. This heterogeneity within the overall trend observed here is difficult to explain. On the one hand, it may be related to the heterogeneity of the patients contributing to this study: all of them had an indication for surgery but a completely different disease history [Table1]. On the other hand, it appeared that beside this aspect the changes of junctional proteins were especially conserved in enteroids when they had been generated from sites of severe inflammation. We observed a downregulation of Dsg2, Claudin4 and 5 as well as an upregulation of pore-forming Claudin2 in the enteroids from the majority of CD patients. In contrast to the original full wall tissue specimens, Claudin1 and E-Cad were unchanged [Table 2]. Based on this it can be assumed that some of the changes that are consistently observed in full wall tissue specimens are memorized on a stem cell level while others appear to occur secondarily (e.g. due to inflammatory stimuli). This idea is supported by a recent study focusing on dysregulated endoplasmatic reticulum stress pathways in enteroids from inflammatory bowel diseases where the authors suggested that prolonged periods of stress signalling may reshape intestinal epithelial stem cells to an inflammatory phenotype.[43] In addition, these and our human data match the observations in colonic organoids from mice showing that chronic inflammation led to lasting changes.[44]

To further investigate this hypothesis resection specimens from patients with CD that are completely uninflamed would be desirable. However, because there is no indication for surgery in this group of patients this was neither possible nor ethical to achieve. An alternative could be to collect endoscopic biopsies from these patients, which has the disadvantage that they derive mostly from the superficial mucosa, which we have found does not allow the generation of enteroids from stem cells.

Interestingly, the permanent pattern of changes was evident on a protein level as revealed by Western blot analyses and immunostaining whereas qRT-PCRs showed no differences on the mRNA levels of these junctional proteins when enteroids from CD patients and healthy patients were compared. Therefore, it can be assumed from our data that the changes of junctional proteins are maintained on a post-transcriptional level. This may explain in part why sequencing of the whole transcriptome in IBD patients has not shown considerable changes of mRNA levels of junctional proteins.[45] Nonetheless it is interesting to note that in patient's samples of naïve ulcerative colitis only Claudin2 was significantly upregulated in whole transcriptome analysis.[46]

In a different context, it has previously been observed in colonoids from patients with ulcerative colitis that the NF-κB signalling pathway was sustained without cytokine stimulation, which was proposed to be related to the carcinogenesis in patients with ulcerative colitis.[44] Dotti *et al*. described that colonic organoids from patients with ulcerative colitis show significant changes in their mRNA expression compared to healthy controls,[47] which in part was also shown for patients with CD.[19] All these data support our present observation that specific changes in CD are maintained on the stem cell level. The novelty of our data is that these conserved changes are maintained on a protein level for several critical junctional proteins over several passages *in vitro*.

The fact that junctional proteins such as E-Cad and Claudin1 are not altered in the enteroids may indicate that some changes in intestinal barrier function are dependent on the presence of inflammatory stimuli whereas others are regulated by other mechanisms. This may explain why different groups have reported different patterns of changes of Claudins and E-Cad[6,26,27,48] in patients with CD. The potential mechanisms underlying the conserved changes of junctional proteins in intestinal stem cells remain unclear at present and will be investigated in detail. The post-transcriptional regulation of junctional proteins independent of transcription is increasingly recognized to contribute to barrier regulation. These mechanisms involve glycosylation, phosphorylation, endocytosis or degradation by the ubiquitin proteasome system.[49] In particular, the ubiquitin proteasome system has previously been shown to be severely affected in IBD.[50] To identify the mechanisms of the phenomenon described here will require in-depth analyses of the post-translational modification of junctional proteins, which was not within the scope of the present study.

We have demonstrated here that enteroids in culture maintain some of the alterations of junctional proteins seen in patients with CD. This was especially the case when enteroids were generated from sites of severe inflammation. However, it must be pointed out that changes on the enterocyte level represent only one of numerous different aspects that contribute to the onset and perpetuation of CD. The interplay between all these components remains poorly understood. Nonetheless, our findings confirm our initial hypothesis that enteroids serve as a valid model to further analyse the mechanisms of changes of intestinal barrier dysfunction in CD.

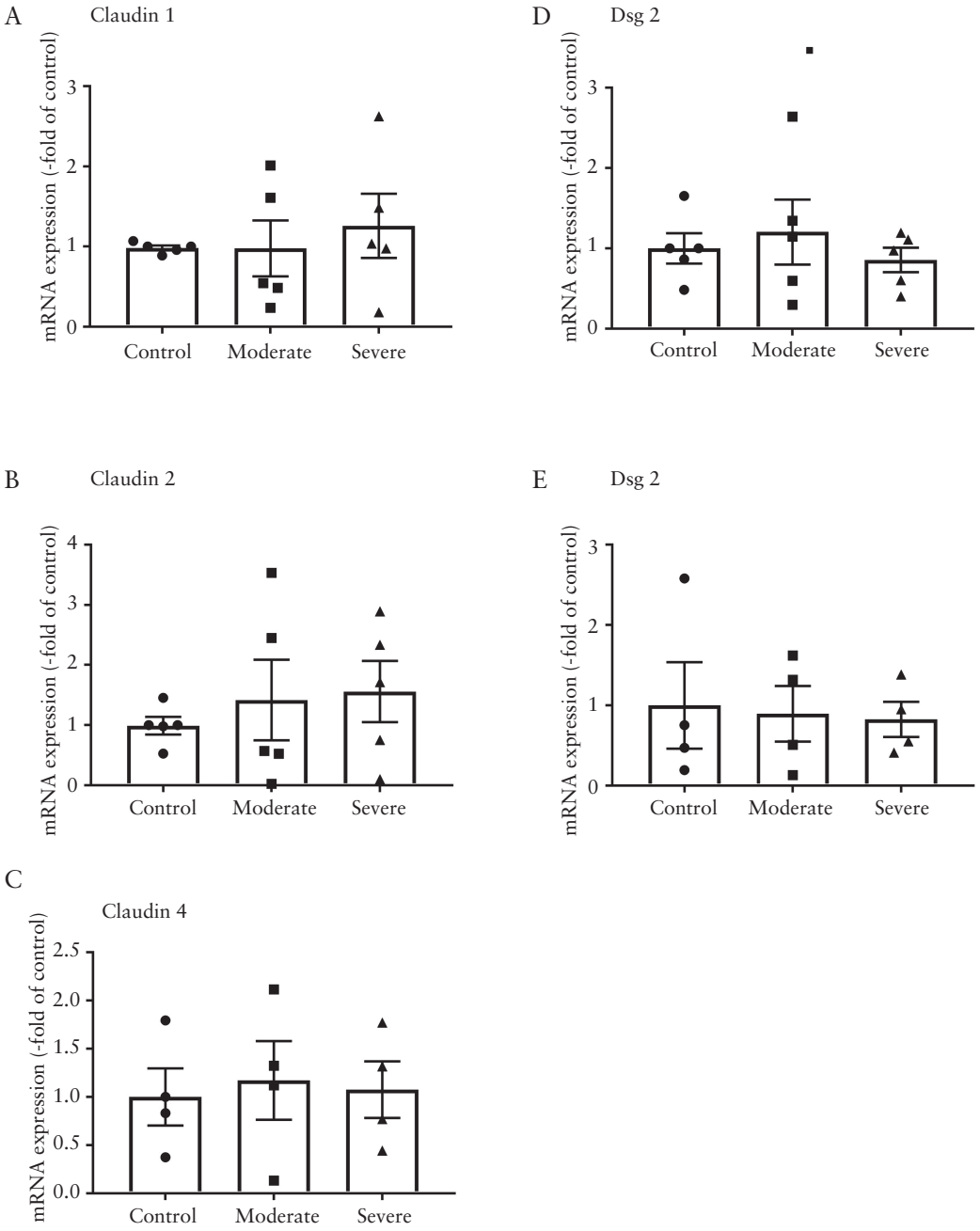

Figure 8. mRNA levels of junctional proteins were not altered in enteroids from CD patients. mRNA expression levels in enteroids from CD patients were quantified by quantitative real-time PCR. Neither tight junction proteins Claudin1, Claudin2, Claudin4 nor desmosomal proteins Dsg2 and Dsc2 were changed in enteroids derived from moderately or severely inflamed terminal ileum compared to non-inflamed healthy controls [$n = 4$; $p < 0.05$].

Funding

This work was supported by the Deutsche Forschungsgemeinschaft [DFG] Priority Programme SPP 1782 grant SCHL1962/5-2 to N.S. and J.W. and by the Interdiszplinaere Zentrum fuer Klinische Forschung [IZKF] Z-2/63 to M.M.

Conflict of Interest

None of the authors has any conflicts of interest to declare.

Acknowledgments

The authors thank Eva Riedel, Veronica Heimbach, Andrea Knorz and Monika Koospal for their technical assistance.

Author Contributions

MM, NB, MaM, NS: study concept, experiments, drafting figures and manuscript. JS, FK: experiments, drafting figures and manuscript. CF, MS, CB: experiments, drafting manuscript. CK, JW, CTG: study concept, drafting manuscript.

Supplementary Data

Supplementary data are available at *ECCO-JCC* online.

References

1. Chang J, Leong RW, Wasinger VC, Ip M, Yang M, Phan TG. impaired intestinal permeability contributes to ongoing bowel symptoms in patients

with inflammatory bowel disease and mucosal healing. *Gastroenterology* 2017;**153**:723–731.e1.
2. Okamoto R, Watanabe M. Role of epithelial cells in the pathogenesis and treatment of inflammatory bowel disease. *J Gastroenterol* 2016;**51**:11–21.
3. Martini E, Krug SM, Siegmund B, Neurath MF, Becker C. Mend your fences: the epithelial barrier and its relationship with mucosal immunity in inflammatory bowel disease. *Cell Mol Gastroenterol Hepatol* 2017;**4**:33–46.
4. Luissint AC, Parkos CA, Nusrat A. Inflammation and the intestinal barrier: leukocyte–epithelial cell interactions, cell junction remodeling, and mucosal repair. *Gastroenterology* 2016;**151**:616–32.
5. Farquhar MG, Palade GE. Junctional complexes in various epithelia. *J Cell Biol* 1963;**17**:375–412.
6. Spindler V, Meir M, Vigh B, *et al*. Loss of Desmoglein 2 contributes to the pathogenesis of Crohn's disease. *Inflamm Bowel Dis* 2015;**21**:2349–59.
7. Gross A, Pack LAP, Schacht GM, *et al*. Desmoglein 2, but not desmocollin 2, protects intestinal epithelia from injury. *Mucosal Immunol* 2018;**11**:1630–9.
8. Meir M, Burkard N, Ungewiß H, *et al*. Neurotrophic factor GDNF regulates intestinal barrier function in inflammatory bowel disease. *J Clin Invest* 2019;**129**:2824–40.
9. Auletta S, Bonfiglio R, Wunder A, *et al*. Animal models for the study of inflammatory bowel diseases: a meta-analysis on modalities for imaging inflammatory lesions. *Q J Nucl Med Mol Imaging* 2018;**62**:78–100.
10. Eichele DD, Kharbanda KK. Dextran sodium sulfate colitis murine model: An indispensable tool for advancing our understanding of inflammatory bowel diseases pathogenesis. *World J Gastroenterol* 2017;**23**:6016–29.
11. Bamias G, Arseneau KO, Cominelli F. Mouse models of inflammatory bowel disease for investigating mucosal immunity in the intestine. *Curr Opin Gastroenterol* 2017;**33**:411–6.
12. Xing T, Camacho Salazar R, Chen YH. Animal models for studying epithelial barriers in neonatal necrotizing enterocolitis, inflammatory bowel disease and colorectal cancer. *Tissue Barriers* 2017;**5**:e1356901.
13. Noben M, Vanhove W, Arnauts K, *et al*. Human intestinal epithelium in a dish: Current models for research into gastrointestinal pathophysiology. *United European Gastroenterol J* 2017;**5**:1073–81.
14. Yui S, Nakamura T, Sato T, *et al*. Functional engraftment of colon epithelium expanded in vitro from a single adult Lgr5$^+$ stem cell. *Nat Med* 2012;**18**:618–23.
15. Sato T, Vries RG, Snippert HJ, *et al*. Single Lgr5 stem cells build crypt-villus structures in vitro without a mesenchymal niche. *Nature* 2009;**459**:262–5.
16. Sugimoto S, Sato T. Establishment of 3D intestinal organoid cultures from intestinal stem cells. *Methods Mol Biol* 2017;**1612**:97–105.
17. Schweinlin M, Wilhelm S, Schwedhelm I, *et al*. Development of an advanced primary human in vitro model of the small intestine. *Tissue Eng Part C Methods* 2016;**22**:873–83.
18. Dotti I, Mora-Buch R, Ferrer-Picón E, *et al*. Alterations in the epithelial stem cell compartment could contribute to permanent changes in the mucosa of patients with ulcerative colitis. *Gut* 2017;**66**:2069–79.
19. Suzuki K, Murano T, Shimizu H, *et al*. Single cell analysis of Crohn's disease patient-derived small intestinal organoids reveals disease activity-dependent modification of stem cell properties. *J Gastroenterol* 2018;**53**:1035–47.
20. Nishimura R, Shirasaki T, Tsuchiya K, *et al*. Establishment of a system to evaluate the therapeutic effect and the dynamics of an investigational drug on ulcerative colitis using human colonic organoids. *J Gastroenterol* 2019;**54**:608–20.
21. Schlegel N, Meir M, Spindler V, Germer CT, Waschke J. Differential role of Rho GTPases in intestinal epithelial barrier regulation in vitro. *J Cell Physiol* 2011;**226**:1196–203.
22. Schlegel N, Waschke J. Impaired integrin-mediated adhesion contributes to reduced barrier properties in VASP-deficient microvascular endothelium. *J Cell Physiol* 2009;**220**:357–66.
23. Truelove SC, Richards WC. Biopsy studies in ulcerative colitis. *Br Med J* 1956;**1**:1315–8.
24. Keita ÅV, Lindqvist CM, Öst Å, Magana CDL, Schoultz I, Halfvarson J. Gut barrier dysfunction-a primary defect in twins with Crohn's disease predominantly caused by genetic predisposition. *J Crohns Colitis* 2018;**12**:1200–9.
25. Landy J, Ronde E, English N, *et al*. Tight junctions in inflammatory bowel diseases and inflammatory bowel disease associated colorectal cancer. *World J Gastroenterol* 2016;**22**:3117–26.
26. Weber CR, Nalle SC, Tretiakova M, Rubin DT, Turner JR. Claudin-1 and claudin-2 expression is elevated in inflammatory bowel disease and may contribute to early neoplastic transformation. *Lab Invest* 2008;**88**:1110–20.
27. Poritz LS, Harris LR 3rd, Kelly AA, Koltun WA. Increase in the tight junction protein claudin-1 in intestinal inflammation. *Dig Dis Sci* 2011;**56**:2802–9.
28. Zeissig S, Bürgel N, Günzel D, *et al*. Changes in expression and distribution of claudin 2, 5 and 8 lead to discontinuous tight junctions and barrier dysfunction in active Crohn's disease. *Gut* 2007;**56**:61–72.
29. Kinugasa T, Akagi Y, Yoshida T, *et al*. Increased claudin-1 protein expression contributes to tumorigenesis in ulcerative colitis-associated colorectal cancer. *Anticancer Res* 2010;**30**:3181–6.
30. Saitou M, Furuse M, Sasaki H, *et al*. Complex phenotype of mice lacking occludin, a component of tight junction strands. *Mol Biol Cell* 2000;**11**:4131–42.
31. Arijs I, De Hertogh G, Machiels K, *et al*. Mucosal gene expression of cell adhesion molecules, chemokines, and chemokine receptors in patients with inflammatory bowel disease before and after infliximab treatment. *Am J Gastroenterol* 2011;**106**:748–61.
32. Muise AM, Walters TD, Glowacka WK, *et al*. Polymorphisms in E-cadherin (CDH1) result in a mis-localised cytoplasmic protein that is associated with Crohn's disease. *Gut* 2009;**58**:1121–7.
33. Kamekura R, Nava P, Feng M, *et al*. Inflammation-induced desmoglein-2 ectodomain shedding compromises the mucosal barrier. *Mol Biol Cell* 2015;**26**:3165–77.
34. Kamekura R, Kolegraff KN, Nava P, *et al*. Loss of the desmosomal cadherin desmoglein-2 suppresses colon cancer cell proliferation through EGFR signaling. *Oncogene* 2014;**33**:4531–6.
35. Ungewiß H, Rötzer V, Meir M, *et al*. Dsg2 via Src-mediated transactivation shapes EGFR signaling towards cell adhesion. *Cell Mol Life Sci* 2018;**75**:4251–68.
36. Ungewiß H, Vielmuth F, Suzuki ST, *et al*. Desmoglein 2 regulates the intestinal epithelial barrier via p38 mitogen-activated protein kinase. *Sci Rep* 2017;**7**:6329.
37. Nava P, Laukoetter MG, Hopkins AM, *et al*. Desmoglein-2: a novel regulator of apoptosis in the intestinal epithelium. *Mol Biol Cell* 2007;**18**:4565–78.
38. Wang H, Li ZY, Liu Y, *et al*. Desmoglein 2 is a receptor for adenovirus serotypes 3, 7, 11 and 14. *Nat Med* 2011;**17**:96–104.
39. Wang H, Ducournau C, Saydaminova K, *et al*. Intracellular signaling and Desmoglein 2 Shedding triggered by human adenoviruses Ad3, Ad14, and Ad14P1. *J Virol* 2015;**89**:10841–59.
40. Bandyopadhyay S, Bonder EM, Gao N. Desmosome disruption by enteropathogenic *E coli*. *Cell Mol Gastroenterol Hepatol* 2018;**6**:225–6.
41. Tran L, Greenwood-Van Meerveld B. Age-associated remodeling of the intestinal epithelial barrier. *J Gerontol A Biol Sci Med Sci* 2013;**68**:1045–56.
42. Torres J, Mehandru S, Colombel JF, Peyrin-Biroulet L. Crohn's disease. *Lancet* 2017;**389**:1741–55.
43. Rees WD, Stahl M, Jacobson K, *et al*. Enteroids derived from inflammatory bowel disease patients display dysregulated endoplasmic reticulum stress pathways, leading to differential inflammatory responses and dendritic cell maturation. *J Crohn's Colitis* 2020;**14**:948–61.
44. Hibiya S, Tsuchiya K, Hayashi R, *et al*. Long-term inflammation transforms intestinal epithelial cells of colonic organoids. *J Crohns Colitis* 2017;**11**:621–30.
45. Planell N, Lozano JJ, Mora-Buch R, *et al*. Transcriptional analysis of the intestinal mucosa of patients with ulcerative colitis in remission reveals lasting epithelial cell alterations. *Gut* 2013;**62**:967–76.
46. Taman H, Fenton CG, Hensel IV, Anderssen E, Florholmen J, Paulssen RH. Transcriptomic landscape of treatment-naïve ulcerative colitis. *J Crohns Colitis* 2018;**12**:327–36.

47. Dotti I, Mora-Buch R, Ferrer-Picón E, *et al*. Alterations in the epithelial stem cell compartment could contribute to permanent changes in the mucosa of patients with ulcerative colitis. *Gut* 2018;**12**:327–36.
48. Karayiannakis AJ, Syrigos KN, Efstathiou J, *et al*. Expression of catenins and E-cadherin during epithelial restitution in inflammatory bowel disease. *J Pathol* 1998;**185**:413–8.
49. Shigetomi K, Ikenouchi J. Regulation of the epithelial barrier by post-translational modifications of tight junction membrane proteins. *J Biochem* 2018;**163**:265–72.
50. Cleynen I, Vazeille E, Artieda M, *et al*. Genetic and microbial factors modulating the ubiquitin proteasome system in inflammatory bowel disease. *Gut* 2014;**63**:1265–74.